Enantioseparation of Chiral Aromatic Acids in Process Intensified Liquid–Liquid Extraction Columns

Alexander Holbach, Julia Godde, Ramanan Mahendrarajah, and Norbert Kockmann
Dept. of Biochemical and Chemical Engineering, Equipment Design, TU Dortmund, Emil-Figge-Straße 68, 44227 Dortmund, Germany

DOI 10.1002/aic.14654
Published online October 28, 2014 in Wiley Online Library (wileyonlinelibrary.com)

Enantioselective liquid–liquid extraction (ELLE) is a powerful alternative to common technologies for separation of racemic mixtures. The first application of ELLE for aromatic acids in liquid–liquid extraction columns is described. The ELLE is investigated experimentally and theoretically for phenylsuccinic acid (PSA) as a representative for aromatic acids. A racemic mixture of (R/S)-PSA is separated with hydroxypropyl-β-cyclodextrin as selector molecule. The ELLE obtained the highest operative selectivity ($\alpha_{op} = 1.8–2$) for low pH-values and temperatures. Because of the low operative selectivity, a countercurrent process is necessary to separate both enantiomers completely. The countercurrent process is investigated in process intensified extraction columns ($Ø_{in} = 15$ mm) with a high number of equilibrium stages. The experiments demonstrate a good symmetric separation with an enantiomeric excess of 60% and yields of 80% for both enantiomers. Finally, the back extraction is investigated to recycle the selector molecule and increase the efficiency. *AIChE J*, 61: 266–276, 2015
Keywords: chiral separation, extraction, separation process, aromatic acids, process intensification

Introduction

Most of the molecules found in the metabolism of humans, animals, and plants are chiral such as amino acids, nucleic acids, and sugars, as well as molecular structures as peptides, proteins, and polysaccharides.[1] Chirality is important for specific interactions of biogenesis and following regulation processes. Chiral molecules enable specific connection with other stereospecific molecules (selector molecules). The interacting molecules have in most cases complex biomolecular structures. (R)- and (S)-enantiomers can interact with selector molecules in totally different ways depending on their stereospecific structure. Consequences for pharmaceuticals are serious; often only one enantiomer is bioactive and causes the desired pharmaceutical effect. The other enantiomer is inactive, has a similar or different pharmaceutical impact or causes side effects. Thus, chiral molecules play an important role for pharmaceuticals, agrochemicals, foods, aromas, and flavors to enable specific effects.[1,2]

Due to the same molecular structure, enantiomers have similar physico-chemical proberties, such as boiling point, solubility, optical spectra, and bonding length. This complicates the separation of both molecules with common distillation, crystallization, or extraction techniques. Generally, there are two methods to separate single enantiomers. The first well-established resolution is the crystallization technology using direct[3] or classical diastereomeric crystallization.[2] Drawback of this separation technique is the expensive and in most cases discontinuous process. Especially, solid handling during crystallization needs additional efforts. The second and high potential alternative is simulated moving bed chromatography. The countercurrent flow between solid and liquid phase is simulated with periodic switching of inlet and outlet positions. Presently, the technology shows a high productivity up to 1–10 kg/(kg_{PM} day).[3] However, chromatography columns are inflexible for multipurpose applications and expensive depending on acquisition and cost of operation. Furthermore, there are several emerging techniques for the separation of racemic mixtures for analytical and preparative applications, such as catalyzed conversion of the racemic mixture to the pure enantiomer,[4,5] membranes,[6–9] capillary electrophorese,[10–12] and the enantioselective liquid–liquid extraction (ELLE).[13–16] Compared to current techniques, the ELLE is a promising alternative to realize a continuous and flexible process.[17,18] Additionally, the extraction in countercurrent flow indicates a higher capacity than chromatography columns.[18] ELLE has a high potential but needs to become more efficient[1] to offer an economical alternative.

Single Stage Enantioselective Liquid–Liquid Extraction

ELLE is based on the selective recognition of one of the enantiomers by a chiral selector molecule. At which the selectivity of the reversible complex reaction defines the quality of the separation process. A high selectivity and the ability to bind a broad range of enantiomer classes are necessary for multipurpose applications. Nowadays, a lot of enantioselective extraction systems are well investigated. Detailed summaries were published in literature.[17,19,20] They show possible separation systems for amino acids, alcohols and

Correspondence concerning this article should be addressed to A. Holbach at alexander.holbach@tu-dortmund.de.

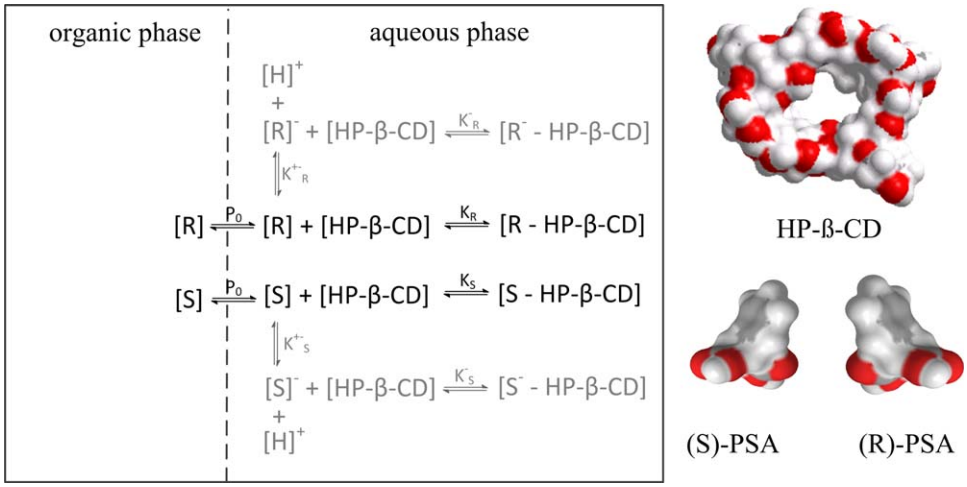

Figure 1. Phenylsuccinic acid (PSA) distribution based on the physical distribution coefficient p_0 and complex reaction with hydroxypropyl-β-cyclodextrin (HP-β-CD); left figure: complex reaction within two phase system; right: Conolly-surfaces of PSA and HP-β-CD.

[Color figure can be viewed in the online issue, which is available at wileyonlinelibrary.com.]

esters, as well as aromatic acids. It could be demonstrated in several works that β-cyclodextrin derivatives have great potential for the ELLE of aromatic acids.[21–26] The mechanism of enantioseparation by cyclodextrin derivatives is schematically shown in Figure 1. The selective extractor, in this case hydroxypropyl-β-cyclodextrin (HP-β-CD), is dissolved in the aqueous phase and insoluble in the organic phase. The physical distribution p_0 of both enantiomers between two phases is equal and unselective. Only the selector molecule enables for an enantioseparation of the two enantiomers, because the complex is preferred with one enantiomer due to steric orientation and interactions. The ELLE of aromatic acids is exemplarily shown in this work for phenylsuccinic acid (PSA). Both enantiomers (R) and (S) fit into the cavitation of the selector molecule, but only the (S)-enantiomer is preferred (see Figure 1 on the right side). At which the selectivity between selector molecule and guest is based on van der Waals forces, hydrogen bonds, and stereospecific interactions. The result is an enrichment of the (S)-enantiomer in the aqueous phase and, consequently an enrichment of the (R)-enantiomer in the organic phase.

The distribution of the two enantiomers at the chemical equilibrium can be calculated using equilibrium constants and distribution coefficients. Tang et al. proved this experimentally for different aromatic acids, for example, cyclohexyl madelic acid[27] and PSA.[28]

The physical distribution p_0 of both enantiomers is described by the ratio of the enantiomer concentrations [R] and [S] within the organic and aqueous phase. It is defined as a function of the enantiomer concentration and the temperature in Eq. 1

$$p_0(C_{R/S};T)=\frac{[R]_{aq}}{[R]_o}=\frac{[S]_{aq}}{[S]_o} \tag{1}$$

Additionally, depending on their acidic character of PSA, both enantiomers dissociate in the aqueous phase. The dissociation equilibrium constant $K^{\pm}$ is shown in Eq. 2 and describes the equilibrium of the reaction. The dissociation is unselective and depends only on the pH value and enantiomer concentrations. Equation 2 can be simplified for the practical system with low concentrations of aromatic acids by assumption of constant activity coefficients γ to one

$$K^{\pm}(C_{R/S};C_{H^+})=\frac{\gamma_{R^-}[R^-]_{aq}\cdot\gamma_{H^+}[H^+]_{aq}}{\gamma_R[R]_{aq}}=\frac{\gamma_{S^-}[S^-]_{aq}\cdot\gamma_{H^+}[H^+]_{aq}}{\gamma_S[S]_{aq}} \tag{2}$$

The selective recognition occurs in the aqueous phase depending on the complex reaction. The chemical equilibrium is described by the equilibrium constants K_R and K_S in Eq. 3. The complex reaction is preferred with undissociated aromatic acids. However, complexes with dissociated acids are possible,[29] too, as it is shown gray shaded in Figure 1 left, but they can be neglected at low pH-values

$$\begin{aligned}K_R(C_{R/S};C_{HP\text{-}\beta\text{-}CD};T)&=\frac{[R-HP-\beta-CD]_{aq}}{[R]_{aq}\cdot[HP-\beta-CD]_{aq}}\\ K_R(C_{R/S};C_{HP\text{-}\beta\text{-}CD};T)&=\frac{[S-HP-\beta-CD]_{aq}}{[S]_{aq}\cdot[HP-\beta-CD]_{aq}}\end{aligned} \tag{3}$$

At low pH values and with an excess of the selector molecule the distribution coefficients are only influenced by the physical distribution and the complex reaction. The overall distribution D_R and D_S at chemical equilibrium can be calculated according to Eqs. 4 and 5

$$D_R=\frac{c_{aq}}{c_o}=p_0\cdot(1+K_R\cdot[HP-\beta-CD]) \tag{4}$$

$$D_S=\frac{c_{aq}}{c_o}=p_0\cdot(1+K_S\cdot[HP-\beta-CD]) \tag{5}$$

Enantioseparation of racemic mixtures are characterized concerning the selectivity of the reactive system. The operative selectivity α_{op} describes the separation efficiency including influences of the process, such as dissociation inside the aqueous phase or physical distribution influences of the aromatic acids. It is defined as the ratio of the distribution coefficients D_S and D_R at the chemical equilibrium. The upper limit of the operative selectivity is determined by the intrinsic selectivity α_{int}. It is described by the ratio of both complex equilibrium constants K_S and K_R. They are shown in Eq. 6

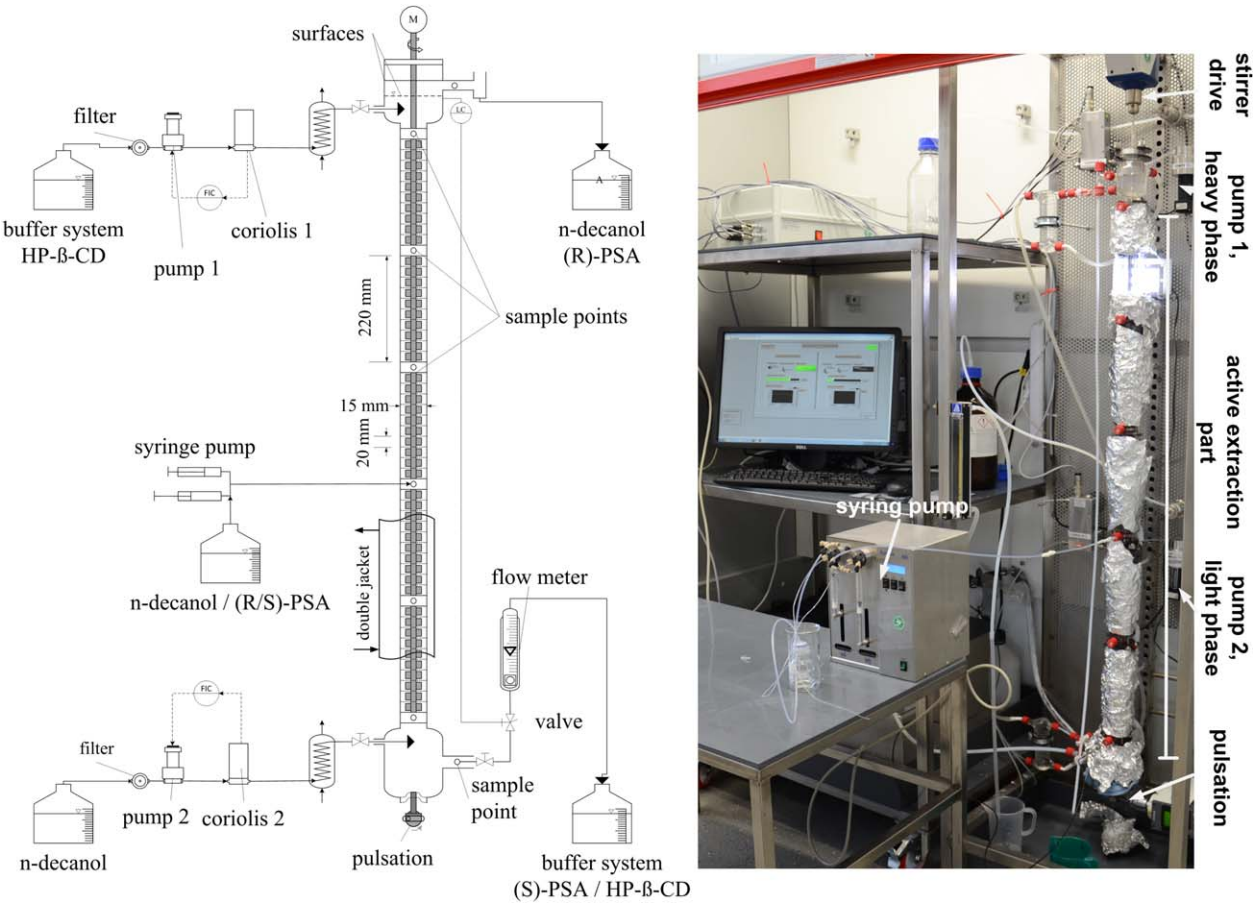

Figure 2. Process intensified extraction column (PIEC) for the fractional extraction; left-hand side: P&ID of the miniaturized extraction column with instrumentation for the fractional extraction; right-hand side: image of the isolated extraction column.

[Color figure can be viewed in the online issue, which is available at wileyonlinelibrary.com.]

$$\alpha_{op} = \frac{D_S}{D_R}; \text{for } D_S > D_R \quad \alpha_{int} = \frac{K_S}{K_R}; \text{for } K_S > K_R \qquad (6)$$

The enantiomeric excess ee is a measure for the purity. It can be calculated for both phases according to Eq. 7

$$ee_{S,aq} = \frac{|[S]_{aq} - [R]_{aq}|}{[S]_{aq} + [R]_{aq}} \quad ee_{R,o} = \frac{|[R]_o - [S]_o|}{[R]_o + [S]_o} \qquad (7)$$

Besides the enantiomeric excess, another important parameter is the yield Y. It is defined for a continuous countercurrent process according to Eq. 8

$$Y_S = \frac{\dot{n}_{S,aq}}{\dot{n}_{S,Feed}} \quad Y_R = \frac{\dot{n}_{R,o}}{\dot{n}_{R,Feed}} \qquad (8)$$

Material and Methods

A racemic mixture of (R/S)-PSA (Alfa Aesar, 98%) is separated inside an organic/aqueous two phase system. The organic phase is *n*-decanol (Alfa Aesar, 98%) and the aqueous phase consists of a buffer system of 0.1 M phosphoric acid (AppliChem, 10% solution), 0.1 M sodium dihydrogen phosphate (VWR Prolabo, 99.8%), and HP-β-CD (Sigma Aldrich, >99%, average molecular weight 1460 g/mol) as selector molecule. The pH value of the aqueous phase is adjusted between pH 2.5 and 4.5. The pH is checked before and after the experiment using a pH-meter (Consort/C3010). Enantiomer concentrations are detected inside the organic phase using a HPLC (Agilent/1120 Compact), a chiral column (Chiral Technologies Europe/Chiralpak® IB), and a UV detector. The mobile phase consists of heptane, ethanol, and THF (97%/3%/0.3% (v:v)).

Process intensified extraction column

The process intensified extraction column (PIEC) used in this work is specified for small-scale applications. The column is self-designed and was constructed at workshops of our department (Biochemical and Chemical Engineering/TU Dortmund). A detailed characterization of the extraction column with the EFCE - test system *n*-butylacetate/acetone/water is published[30] and compares the new PIEC with conventional miniplant columns. The column has a heating/cooling jacket and is isolated to ensure constant internal temperature. The temperature is controlled using a cryostat (Huber, ministat) and a temperature sensor inside the active extraction area. The inner diameter of the active extraction part is $Ø_{in} = 15$ mm. The active extraction area consists of five modular sections. Each section has 10 stirred cells and an active extraction height of 220 mm. Samples can be taken between each section, which enable measurements of concentration profiles and additional feeds to be led into the active extraction area. The P&ID for the fractional extraction and an illustration of the whole setup are shown in Figure 2. The energy input into the column is a combination of stirring

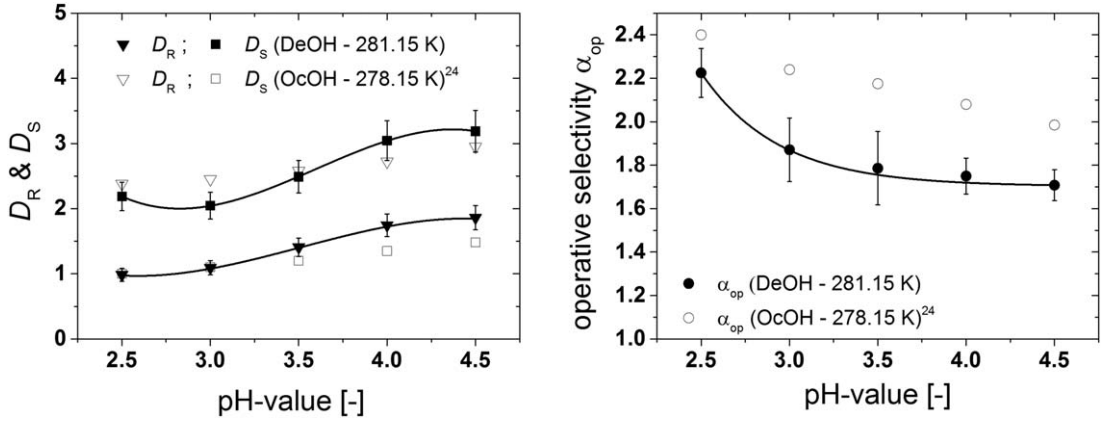

Figure 3. pH influence for the ELLE of PSA, left figure: distribution coefficients D_R and D_S; right figure: operative selectivity α_{op} of PSA – HP-β-CD; DeOH: [(R/S)-PSA] = 1 mmol/L and [HP-β-CD] = 25 mmol/L; OcOH: [HP-β-CD] = 100 mmol/L.

and pulsation. Pulsation of the liquid–liquid system is introduced by using an eccentric drive acting on a flexible membrane at the bottom of the column. Flooding of single stirred cells and the total column is prevented by pulsation of the liquid–liquid system. This new technique allows for the miniaturization of extraction columns and enables a well-controlled countercurrent flow. Countercurrent operation without pulsation is not possible in this miniaturized extraction column. The frequency of pulsation is adjusted from 0.2 to 0.83 Hz. The stroke length h_s of the eccentric drive is constant ($h_s = 5$ mm) during all experiments.

For the countercurrent extraction, the organic and aqueous phase are introduced into the column with micro gear pumps (HNP Mikrosysteme, MZR 7255), while the mass flow rates are controlled (Bronkhorst, Minicoriflow). The aqueous phase is pumped into the column at the top and the organic phase is pumped into the bottom of the column. The mass flow rates are controlled with LabView®. An additional feed (*n*-decanol/(R/S))-PSA) for fractional extraction experiments is realized with a syringe pump (HiTec Zang, SyrDos2).

Chemical equilibrium and countercurrent flow experiments

For the chemical equilibrium experiments, 2.5 mL of the aqueous and organic phase were mixed and hold on constant temperature for 24 h. Depending on the experiment, the temperature was varied between 281.15 and 323.15 K. Both phases were separated after equilibration of the system. The concentrations of (R)- and (S)-enantiomers in the organic phase were analyzed. Concentrations in the aqueous phase were calculated by closing the mass balance. All experiments were performed as duplicates to identify errors of the procedure and analyses.

Continuous countercurrent flow experiments were carried out inside the PIEC. Temperature and pH value for the fractional extraction experiments were constant at 281.15 K and pH 2.5. The feed volume flow rate was 0.2 mL/min *n*-decanol with 50 mmol/L (R/S)-PSA. The pure organic (*n*-decanol) and the aqueous volume flow rate (buffer system with 25 mmol/L HP-β-CD) were 4.8 and 4 mL/min, respectively. The aqueous phase with the selector molecule and enriched (S)-PSA was collected during the steady state after the fractional extraction and injected into the back extraction (4 mL/min aqueous phase together with 4.8 mL/min pure *n*-decanol). The back extraction is carried out at 323.15 K and same pH value of 2.5.

Equilibrium studies of the enantioselective extraction

Influence of pH Influence on the Chemical Equilibrium. The solubility of aromatic acids in the aqueous phase is controlled by different pH values. It influences the dissociation equilibrium, which is defined in Eq. 2. At low pH values, the nondissociated form is present. This results in decreased solubility of PSA in the aqueous phase and hence decreased distribution coefficients. Figure 3 on the left-hand side shows the distribution coefficients D_R and D_S at constant selector molecule concentrations and a constant temperature. The distribution coefficients increase for PSA with higher pH values. Increased solubility of the enantiomers in the aqueous phase increases the distribution coefficients of PSA. Our measurements with *n*-decanol (DeOH) are compared to data from Tang et al.,[24] who used *n*-octanol (OcOH) as organic solvent. Octanol allows for conducting the experiments at lower temperatures. Nevertheless, a significant difference to the literature is the primarily extracted enantiomer with HP-β-CD. In contrast to the literature,[24,28] our measurements indicate that the (S)-enantiomer is prefered for the complex reaction, when using pure enantiomers. The difference has to be checked detailed in further investigations.

However, the tendency and dimension of the distribution coefficients are the same. The comparison shows a reduced selector molecule concentration for *n*-decanol as organic solvent. Equivalent distribution coefficients are realized with 25 mmol/L selector molecule instead of 100 mmol/L for *n*-octanol. Differences are based on the changed physical distribution coefficients of PSA in the organic/aqueous two phase systems and different concentration areas of PSA.

To enable a complete separation of both enantiomers, it is important to achieve a high operative selectivity, defined in Eq. 6. Figure 3 on the right-hand side illustrates the operative selectivity in dependency of the pH value. The operative selectivity decreases with increasing pH values. For low pH values, the dissociation is negligible. The comparison of both organic phases indicates a higher selectivity for octanol. A lower temperature and a more suitable physical distribution coefficient for octanol allow for more selective complex inclusions in the aqueous phase. A higher operative

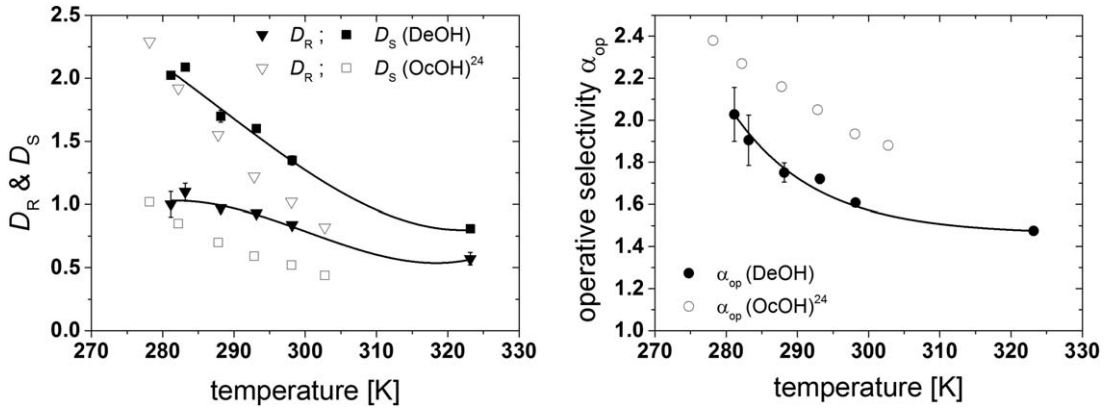

Figure 4. Temperature influence for the ELLE of PSA, left figure: distribution coefficients D_R and D_S; right figure: operative selectivity α_{op} of PSA – HP-β-CD; DeOH: [(R/S)-PSA] = 1 mmol/L and [HP-β-CD] = 25 mmol/L; OcOH: [HP-β-CD] = 100 mmol/L.

selectivity can be realized, but the intensification has to be paid with higher amounts of the selector molecule.

Temperature Influence on the Chemical Equilibrium. The temperature effects the stability of the complex and has direct influence on both, the intrisic and operative selectivity. Depending on the exothermic complex reaction, the complex is more unstable at higher temperatures and less complexes can be formed in the aqueous phase. The distribution coefficients decrease with increasing temperature. Figure 4 (on the left side) shows this effect for both distribution coefficients, D_R and D_S. The distribution coefficients decrease from 281.15 to 323.15 K. Figure 4 (on the right side) shows the corresponding operative selectivity of the systems. The operative selectivity decreases from 281.15 to 323.15 K. The minimum temperature for extraction is given by the melting point of the organic solvent, in this case 279.85 K for *n*-decanol.[31] Hence, the temperature is set to 281.15 K for the following experiments.

As already shown for the pH values, the comparison of both organic solvents indicates nearly the same tendency for the temperature influence, but a higher operative selectivity for *n*-octanol. Nevertheless, a higher operative selectivity requires four times higher selector molecule concentrations.

Concentration Influence of the Selector Molecule on the Equilibrium. The operative selectivity in dependence of aromatic acid (PSA) and selector molecule concentrations (HP-β-CD) is demonstrated in Figure 5. Temperature and pH value are kept constant at 281.15 K and 2.5, respectively. The operative selectivity indicates a high value over a broad concentration range. The average operative selectivity is around 1.8–2. To enable for a high operative selectivity, a minimum selector molecule concentration of 20 mmol/L is necessary. The high values decrease for aromatic acid concentrations smaller 0.5 mmol/L and high concentrations of the selector molecule. This tendency is based on the excess of the selector molecule. A high excess of the selector molecule enable more and unselective complexes.

The selector molecule excess SE is defined by the molar ratio between the selector molecule and the racemic mixture

$$\mathrm{SE} = \frac{[\mathrm{HP}-\beta-\mathrm{CD}]}{[\mathrm{R}]+[\mathrm{S}]} \tag{9}$$

The chosen initial condition for the countercurrent extraction indicates a selector molecule excess of SE = 10. The selector molecule concentration has a direct influence on the distribution coefficients D_R and D_S, which is demonstrated in Figure 6. Higher concentrations of HP-β-CD increase the distribution coefficients. More complexes are generated inside the aqueous phase. Nevertheless, D_R increases as well and also more unselective complexes exist inside the aqueous phase. The system indicates a linear behavior of the distribution coefficients depending on the selector molecule concentration. The impact of the racemate concentration is rather small within this concentration range. However, (R/S)-PSA concentrations smaller 0.5 mmol/L indicate reducing distribution coefficients.

The selector molecule concentration for fractional extraction is estimated in this work based on the extraction factor. A good separation during fractional extraction is expect for an extraction factor smaller than one for the (R)-enantiomer and higher than one for the (S)-enantiomer. Large differences are not desired and implicate increasing phase ratios, which are not possible or not economical in extraction columns. A first estimation for the volume flow rates of organic ($\dot{\mathrm{R}}$/raffinate) and aqueous phase ($\dot{\mathrm{E}}$/extract) is following with Eqs. 10 and 11

$$\frac{D_R}{\dot{\mathrm{R}}/\dot{\mathrm{E}}} < 1; \qquad \frac{D_S}{\dot{\mathrm{R}}/\dot{\mathrm{E}}} > 1 \tag{10}$$

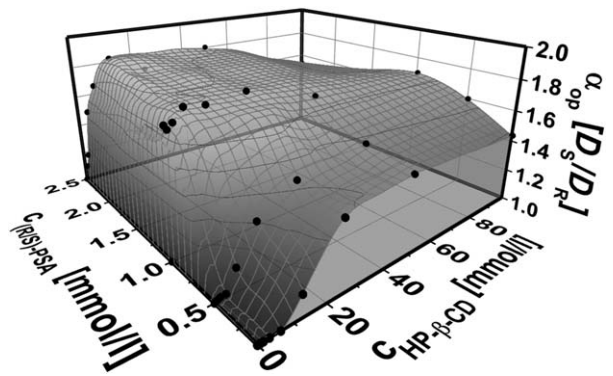

Figure 5. Concentration influences of the racemic mixture (R/S)-PSA and the selector molecule HP-β-CD concentrations for the operative selectivity α_{op}; T = 281.15 K; pH = 2.5; • measured points.

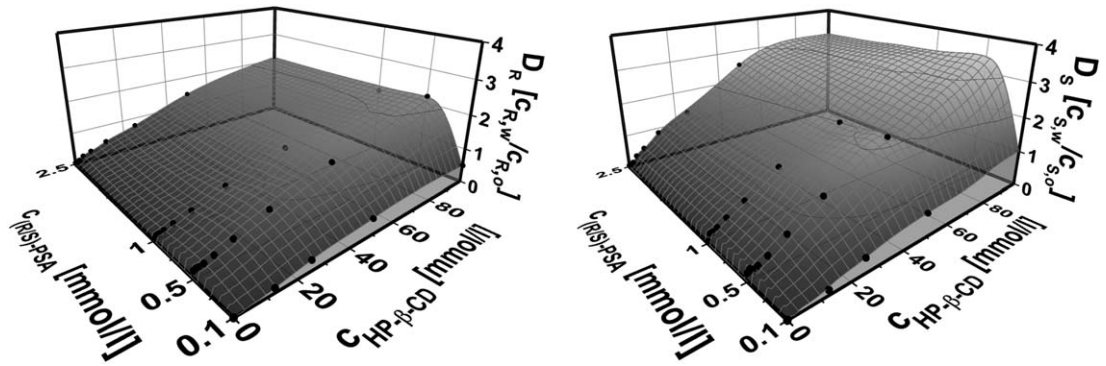

Figure 6. Concentration influences of the racemic mixture (R/S)-PSA and the selector molecule HP-β-CD concentrations for the distribution coefficients D_R (left figure) and D_S (right figure); $T = 281.15$ K; pH 2.5; • measured points.

$$\dot{R}/\dot{E} \approx \sqrt{D_R \cdot D_S} \tag{11}$$

Considering countercurrent applications, the HP-β-CD concentration should not exceed 30 mmol/L and go below 15 mmol/L to prevent extreme volume flow rates.

Simulation of the distribution coefficients

The distribution coefficients can be calculated for low pH values over a broad concentration range using Eqs. 4 and 5. Dissociation of the aromatic acids and the formation of additional complexes with the dissociated PSA are neglected for low pH values. Temperature influences on the complex between the aromatic acids and the selector molecule are mainly described by the equilibrium constants K_R and K_S, respectively. The equilibrium constants $K_R = 168.2$ L/mol and $K_S = 379.9$ L/mol are calculated for 281.15 K, which results in an intrinsic selectivity of $\alpha_{int} = 2.26$. The concentration influence on the physical distribution coefficient p_0 is described within the concentration range for PSA using the correlation in Eq. 12

$$p_0 = -0.019 \cdot \ln([(R/S)]) + 0.179; \quad \text{for } [(R/S)] : \left(0.1 - 2.5 \frac{\text{mmol}}{\text{L}}\right) \tag{12}$$

Measured distribution coefficients of PSA are compared to calculated results for the chemical equilibrium defined in Eqs. 4 and 5. Figure 7 shows the parity plots of both distribution coefficients. Generally, good predictions are possible with an error less than 17%. They are mainly based on the molecular mass distribution of the selector molecule and concentration influences on the physical distribution coefficients. Small concentrations of PSA (smaller 0.5 mmol/L) and a high selector molecule excess increase the deviation.

Enantioselective liquid–liquid extraction in countercurrent flow

The ELLE was investigated in countercurrent flow during the past years in different devices, such as membranes[7–9] and centrifugal extractors.[32–35] But the high amount of required extraction stages for a complete separation demonstrates the necessity of efficient equipment with many equilibrium stages. Different to previous works, the countercurrent extraction is here for the first time implemented in extraction columns. High number of equilibrium stages inside PIECs supports the separation efficiency of ELLE systems with a low operative selectivity. PIECs indicate depending on small volume flow rates a good option for small-scale operations and process development.

Hydrodynamics inside the process intensified column

In kinetic studies using a Nernst cell, Steensma et al.[36] and Zhang et al.[37] indicated that the ELLE of amino acids and aromatic acids can be described by a fast reaction. The limitation of the complex reaction is only based on the mass transfer of enantiomers over the liquid–liquid interface. For mass transport limited systems, it is important to increase the mass transfer with high specific surfaces, which is generated by high stirrer speeds. Nevertheless, backmixing of the continuous phase will increase as well. To reduce backmixing, the stirred cells have to be separated with stator plates, at which, flooding is prevented by pulsation of the liquid–liquid system. The hydrodynamics inside the active extraction part of the column is investigated at different stirrer speeds of 700, 800, 900, and 1000 rpm and a constant pulsation frequency of 0.83 Hz. Depending on the optically analysis of a sample of 450 droplets with ImageJ®, the Sauter mean diameters d_{32} are calculated according to Eq. 13. The organic phase hold-up ε of the active extraction part is measured by gauging the total volume of the column during the steady state. The specific surface S/V (surface per volume

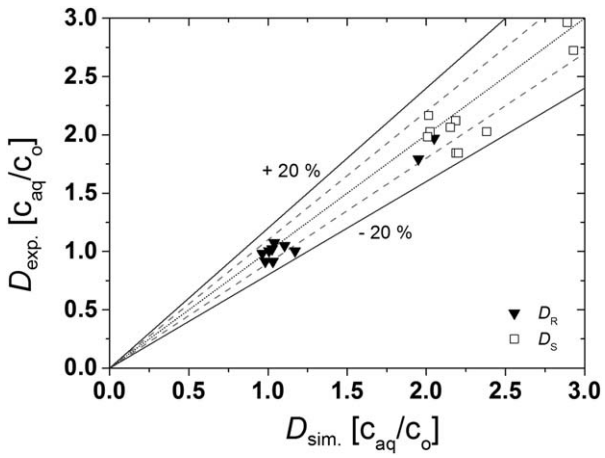

Figure 7. Simulated and experimental distribution coefficients of PSA: D_R and D_S; $T = 281.15$ K; pH 2.5; for [(R/S)-PSA] = 0.5–2.5 mmol/L and [HP-β-CD] = 12.5–100 mmol/L.

Table 1. Hydrodynamic Parameters of the Stirred Cells at Different Stirrer Speeds

rpm	d_{32} (mm)	ε (%)	S/V (m^2/m^3)
700	0.87	9.63	664
800	0.83	12.97	938
900	0.74	15.68	1271
1000	0.76	17.39	1373

ratio) is calculated in respect to the Sauter mean diameter and the hold-up. The results are shown in Table 1

$$\varepsilon = \frac{V_d}{V_d + V_c} \cdot 100\%; \quad d_{32} = \frac{\Sigma N \cdot d^3}{\Sigma N \cdot d^2}; \quad \frac{S}{V} = \frac{6}{d_{32}} \frac{V_d}{V_d + V_c} \quad (13)$$

Higher stirrer speeds generate an increasing hold-up, smaller droplets, and high specific surfaces, as expected. Small droplet diameters and high specific surfaces support mass transport limited systems. The highest specific surface of 1373 m^2/m^3 is observed at 1000 rpm.

A more detailed description than the Sauter mean diameter is given by the droplet size distribution q_0. The droplet size distribution for different stirrer speeds inside PIECs is shown in Figure 8. Generally, lower stirrer speeds generate broader and higher stirrer speeds generate narrower droplet size distributions. Narrow droplet size distributions have a positive effect on back mixing and entrainment of the dispersed phase, because all droplets almost have the same physical buoyancy forces. The tendency between stirrer speed and droplet size distribution within the investigated range is rather small. Narrow droplet size distributions can be expected for all investigated stirrer speeds. With respect to the mass transport limitation and the necessarily high specific surface, high stirrer speeds of 900–1000 rpm will support the ELLE in countercurrent flow.

Fractional extraction of aromatic acids

The fractional extraction of the ELLE is investigated inside PIECs. A racemic mixture of PSA is separated using a stripping and a washing section. The racemic mixture is dissolved in the oganic feed and introduced between the second and third section (height: 440 mm from the bottom) as shown in Figure 2. Within the stripping section, the (S)-enantiomer is extracted out of the organic phase, but depending on the low operative selectivity also the (R)-enantiomer is extracted. The washing section washes the less preferred (R)-enantiomer back. An integrated washing section purifies the (S)-enantiomers in the aqueous phase as well as increase the (R)-enantiomer yield in the organic phase. The measured and simulated concentration profiles inside the active extraction area for PSA are shown in Figure 9. The dashed and solid lines represent the simulated concentration profiles of the organic and aqueous phase, respectively. The simulation is based on the backflow model[38,39] with implemented ELLE equilibrium stages defined in Eqs. 1–5. Experimental data of the measured concentrations of the organic phase are given as well. The highest concentrations of the enantiomers can be observed on the feed stage. Under ideal conditions and enough equilibrium stages, both enantiomers are completely separated. The concentration profiles are compared in Figure 9 for different pulsation frequency. A lower frequency improves the ELLE inside the column drastically. Generally, the pulsation in this column type is necessary to inhibit flooding inside the active extraction area and to destroy the coalescence area. Lower frequencies increase the retention time of the dispersed phase and decrease the backmixing, which results in a better extraction efficiency. The maximum extraction efficiency can be expected with low pulsation frequencies. But the frequency should be high enough to enable a countercurrent flow. The combination of stirring and pulsation allows for a high specific surface within the stirred cells and thus good mass-transfer rates, long retention times, and a reduced backmixing between the cells.

Depending on the missing information of stirring and pulsation influences on the backflow model, the backmixing inside the PIEC is fitted to experimental data of a countercurrent flow reference experiment. The fitting indicates a back mixing of 20% of the total volume flow rates between each stage. The number of calculated equilibrium stages s is adjusted by the outlet concentrations of the top and bottom phase. The backflow model is calculated for both enantiomers assuming equilibrium stages defined in Eqs. 1–5. The calculation assuming equilibrium stages is a simplification of the real behavior inside the extraction column, but gives a good tendency despite its simplicity. The stripping part is well represented, but the washing part shows deviations.

The enantiomeric excess and the yield of both outlets during the steady state are shown more detailed in Table 2. By

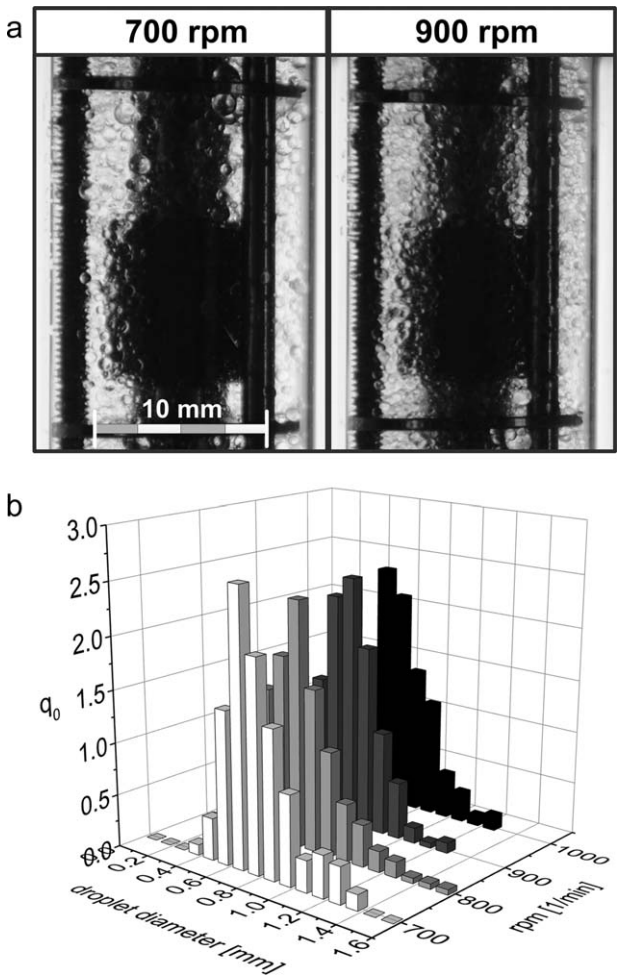

Figure 8. Liquid–liquid system inside the stirred cell; (a) picture of a stirred cell with stirrer speed of 700 and 900 rpm; (b) droplet size distribution q_0 for different stirrer speeds; $T = 281.15$ K, $V_o = 4.8$ mL/min, $V_w = 4.0$ mL/min, $f = 0.83$ Hz.

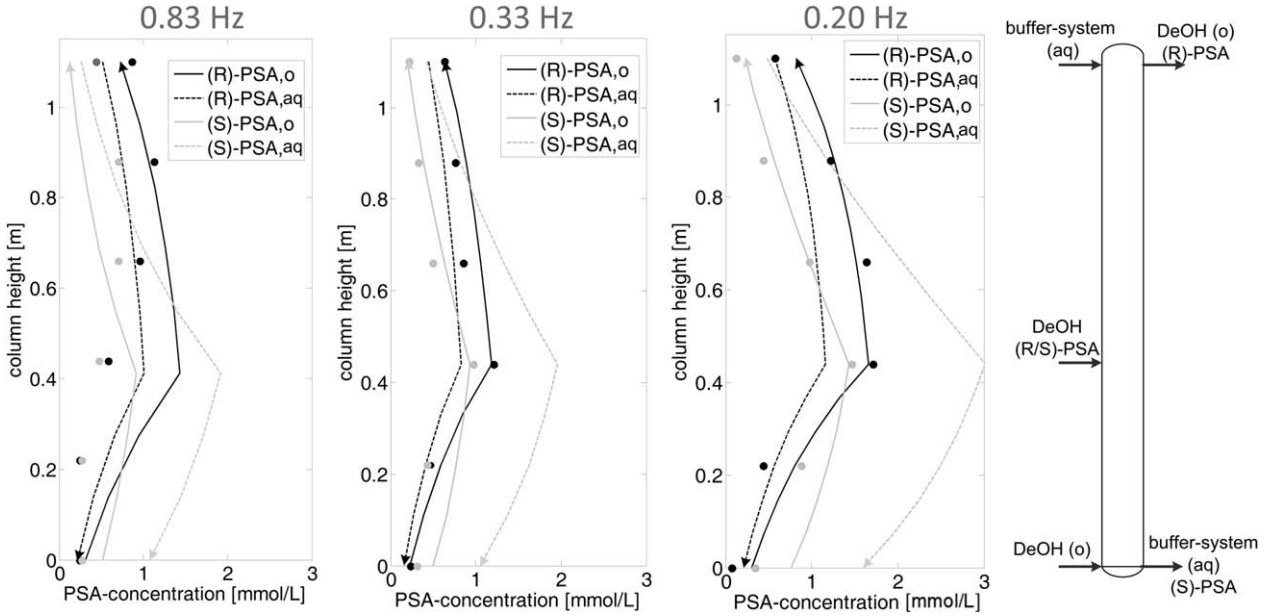

Figure 9. Experimental and simulated concentration profiles using fractional extraction with different pulsation frequencies, $V_o = 4.8$ mL/min, $V_w = 4$ mL/min, $V_{feed} = 0.2$ mL/min, $[(R/S)\text{-PSA}]_{feed} = 50$ mmol/L; [HP-β-CD] = 25 mmol/L; initial SE = 10; $T = 281.15$ K, stirrer speed = 900–1000 rpm; ● measured (R)-enantiomer in the organic phase; ● measured (S)-enantiomer in the organic phase; simulation: backflow ~ 20%; simulated equilibrium stages s: (0.83 Hz → $s = 7$; 0.33 Hz → $s = 10$; 0.2 Hz → $s = 15$).

reducing the pulsation frequency from 0.83 to 0.2 Hz, the enantiomeric excess and yield increase to 60 and 80%, respectively. The benchmark for the fractional extraction of PSA is given by centrifugal extractors. Tang et al.[35] used 10 centrifugal extractors, which represented nearly 10 equilibrium stages. They obtained an enantiomeric excess for symmetric separations of nearly 50% and yields of 75%. This shows that the column with 1.1 m active extraction part has a better performance than 10 centrifugal extractors. The ELLE simulations indicate that the PIECs provide between 7 and 15 equilibrium stages, but with a backflow of 20% between each stage.

Fractional extraction of aromatic acids combined with back extraction

The outlet streams after the fractional extraction indicate an enriched (R)-enantiomer in the organic stream and an enriched (S)-enantiomer complex in the aqueous phase. The selector molecule has to be separated from the (S)-enantiomer and recycled for the fractional extraction to enable an economical process. Considering pH and temperature influences, back extraction can be realized by changing process parameters. The temperature shift is preferred for this system without destroying the buffer system. A temperature shift from 281.15 K for the fractional extraction to 323.15 K for the back extraction leads to distribution coefficients smaller than one and enables for a good separation of the (S)-enantiomer from the selector molecule. Increasing Brownian motion of the molecules by higher temperatures lowers the intermolecular interactions within the complex. The distribution coefficients allow for high concentrations in the organic phase and low concentrations in the aqueous phase.

Table 2. Pulsation Influence on the Fractional Extraction of PSA Inside PIECs

Frequency (Hz)	$ee_{R,org}$	$Y_{R,org}$	$ee_{S,aq}$	$Y_{S,aq}$
0.83	0.41	0.66	0.36	0.73
0.33	0.48	0.64	0.36	0.78
0.20	0.62	0.78	0.57	0.82

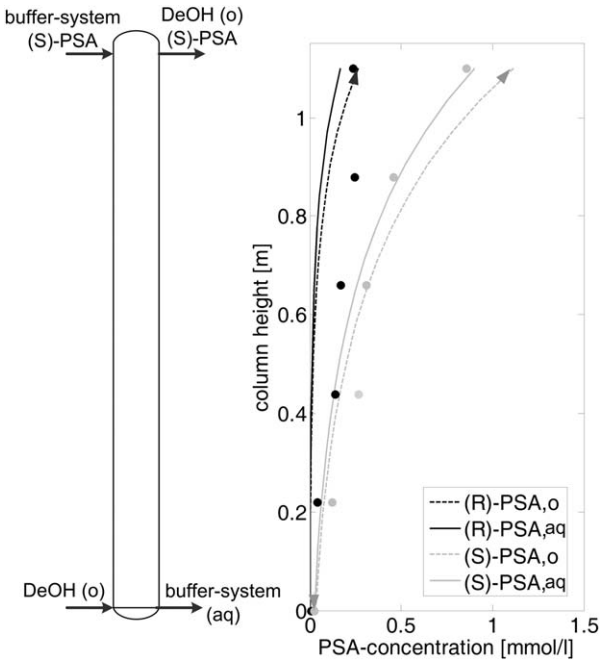

Figure 10. Experimental and simulated concentration profiles of the back extraction, $V_o = 4.8$ mL/min, $V_w = 4$ mL/min, [HP-β-CD] = 25 mmol/L; ● measured (R) enantiomer in the organic phase; ● measured (S) enantiomer in the organic phase; $T = 323.15$ K; $n_s = 1000$ rpm, $f = 0.2$ Hz; simulation: backflow ~ 20%; $s = 20$.

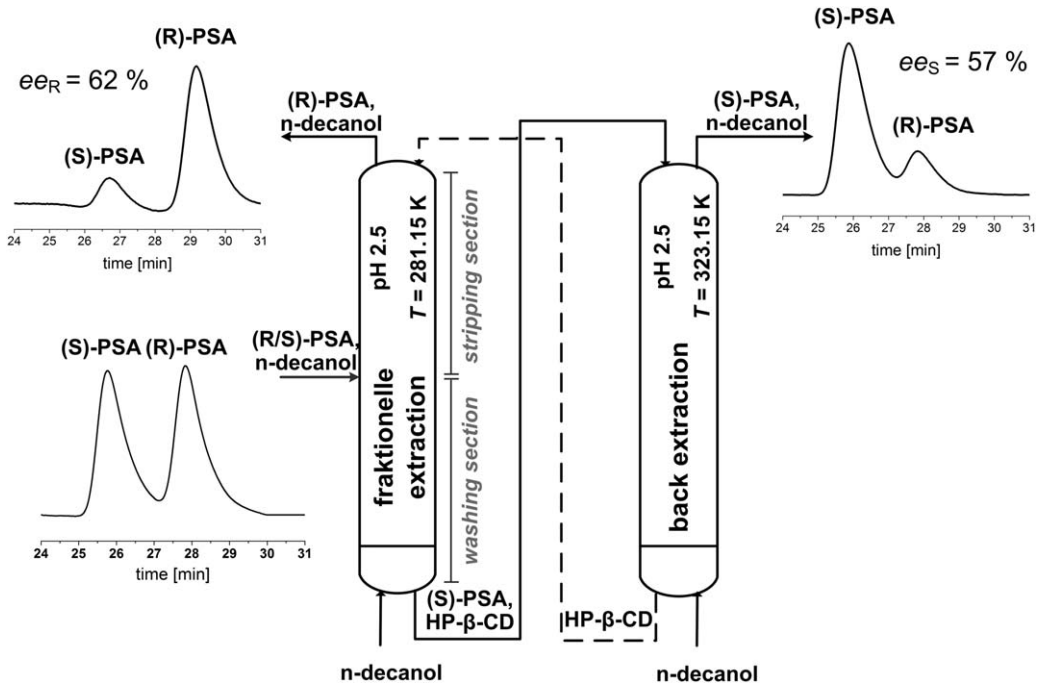

Figure 11. Downstream process of the ELLE with fractional extraction and back extraction, $n_s = 1000$ rpm, $f = 0.2$ Hz, $V_o = 4.8$ mL/min, $V_w = 4$ mL/min, $V_{feed} = 0.2$ mL/min, [HP-β-CD] = 25 mmol/L, $[(R/S)\text{-PSA}]_{feed} = 50$ mmol/L.

The back extraction is investigated experimentally and theoretically. During the experiment, the buffer system with (S)-PSA and HP-β-CD is collected at steady state of the fractional extraction and used for the back extraction. The column used for the back extraction is the same as already used for the fractional extraction with an active extraction height of 1.1 m. The buffer system containing the complex is introduced at the top of the column and pure *n*-decanol phase at the bottom of the column.

Concentration profiles of PSA in the organic phase and the concentration of PSA at the organic outlet stream during the steady state were measured. The back extraction is demonstrated for the fractional extraction with a pulsation frequency of 0.2 Hz. The concentration profile in Figure 10 indicates a satisfying extraction of PSA from the aqueous buffer system into the organic phase. The concentration of PSA decreases from the top to the bottom of the column. Finally, the enantiomer concentration in the aqueous phase is nearly zero. The purification of the selector molecule in the buffer system is checked and confirmed by consideration of the pH-value and reproducibility of the operative selectivity to aromatic acids.

The HPLC-chromatograms of the outlet streams in Figure 11 demonstrate the separation of racemic PSA using an ELLE-downstream process by fractional extraction and recycling of the selector molecule. The process is shown here for the best pulsation frequency ($f = 0.2$ Hz). Both enantiomers indicate the same concentrations at the inlet of the fractional extraction. The (R)-enantiomer is measured with a high enantiomeric excess and yield ($ee_R = 62\%$; $Y_R = 78\%$) in the organic outlet stream after the fractional extraction and the purified (S)-enantiomer is ($ee_S = 57\%$; $Y_S = 82\%$) in the organic outlet stream after the back extraction. The buffer system of pH 2.5 and the selector molecule HP-β-CD are recycled for the fractional extraction. The mass balance for both enantiomers shows an relative error less than 5% and is within the measurement tolerance. A further purification of both enantiomers using the ELLE is possible and requires more separation stages, which is given by a higher column for the fractional extraction. The back extraction dramatically increases the efficiency and economic sustainability of the process due to reuse of the expensive selector molecule (HP-β-CD).

Summary and Outlook

The ELLE in PIECs has high potential to separate racemic mixtures with high efficiency. The PIECs provide up to 15 equilibrium stages for the fractional extraction and enable a separation process of despite a low operative selectivity of the chemical system. The ELLE was demonstrated with a racemic mixture of PSA as an example for aromatic acids. Equilibrium studies indicate that low pH-values and low temperatures are preferred to achieve a high operative selectivity. A defined concentration range of the selector molecule and the racemic mixture is important to maintain a high operative selectivity and good distribution coefficients for the countercurrent process. The fractional extraction inside PIECs shows a good separation efficiency. Both enantiomers are separated with an enantiomeric excess of up to 60% and yields up to 80%. More stages or a higher operative selectivity will increase the separation performance. Using the countercurrent extraction model, 41 equilibrium stages or 3 m active extraction part were determined to separate both enantiomers completely.

A low pulsation frequency of 0.2 Hz enables more equilibrium stages and a better extraction efficiency due to reduced back mixing and longer retention times of the dispersed phase inside the fractional extraction column. The simulation of the fractional extraction indicates a good trend, but will be improved by a more detailed focus on hydrodynamics considering droplet size distribution and kinetic influences on the complex reaction.

Recycling of selector molecule and the buffer system was realized by combining fractional and back extraction. The back extraction is possible by increasing temperature, which

decreases the complex interaction and enables complete separation of (S)-PSA from the selector molecule. It is the first time that a back extraction based on a temperature shift is demonstrated for the enantioseparation of PSA. Accumulation of impurities and the necessity of purging and refreshing have to be checked for industrial applications of ELLE.

Acknowledgment

The authors would like to thank Mr. Carsten Schrömges (BCI/TU Dortmund) for his technical assistance and Mr. Jan Mündges (BCI/TU Dortmund) for the constructive discussion during the project.

Notation

Abbreviations and symbols

DeOH = *n*-decanol
ELLE = enantioselective liquid–liquid extraction
HP-β-CD = hydroxypropyl-β-cyclodextrin
OcOH = *n*-octanol
PIEC = process intensified extraction column
PSA = phenylsuccinic acid
P&ID = process and instrumentation diagram
UV = ultraviolet
D_R = distribution coefficient
D_S = distribution coefficient
d_{32} = Sauter mean diameter, mm
ee_S = enantiomeric excess of the S enantiomer
ee_R = enantiomeric excess of the R enantiomer
f = frequency, Hz
h_s = stroke length, mm
$K^{\pm}$ = dissociation equilibrium constant, mol/L
K_R = complex equilibrium constant, L/mol
K_S = complex equilibrium constant, L/mol
N = number
o = organic phase
p_0 = physical distribution coefficient
s = stages
S = surface, mm^2
SE = selector molecule excess
T = temperature, K
V = volume, mm^3
V_w = volume flow rate aqueous phase, mL/min
V_o = volume flow rate organic phase, mL/min
V_{feed} = volume flow rate feed, mL/min
w = water/aqueous buffer system
Y_S = yield of the S enantiomer
Y_R = yield of the R enantiomer
α_{op} = operative selectivity
α_{int} = intrinsic selectivity
γ = activity coefficient
ε = hold up, %
$Ø_{in}$ = inner diameter, mm

Literature Cited

1. Maier NM, Franco P, Lindner W. Separation of enantiomers: needs, challenges, perspectives. *J Chromatogr A*. 2001;906:3–33.
2. Lien A, Nguyen H-H, Chuang P-H. Chiral drugs: an overview. *Int J Biomed Sci*. 2006;2(2):85–100.
3. Lorenz H, Seidel-Morgenstern A. Verfahren zur Enantiomertrennung. *Angew Chem*. 2014;126:1240–1274.
4. Ganapati DY, Sivakumar P. Enzyme-catalysed optical resolution of mandelic acid via RS(+/-) methyl mandelate in non-aqueous media. *Biochem Eng J*. 2004;19:101–107.
5. Reetz MT, Schimossek K. Lipase-catalyzed dynamic kinetic resolution of chiral amines: use of palladium as the racemization catalyst. *Int J Chem*. 1996;50(12):668–669.
6. Keurentjes JTF, Nabuurs LJWM, Vegter EA. Liquid membrane technology for the separation of racemic mixtures. *J Membr Sci*. 1996; 113(2):351–360.
7. Ding HB, Carr PW, Cussler EL. Racemic leucine separation by hollow-fiber extraction. *AIChE J*. 1992;38:1493–1498.
8. Wang Z, Cai C, Lin Y, Bian Y, Guo H, Chen X. Enantioselective separation of ketoconazole enantiomers by membrane extraction. *Sep Purif Technol*. 2011;79:63–71.
9. Nakamura M, Kiyohara S, Saito K, Sugita K, Sugo T. Chiral separation of dl-tryptophan using porous membranes containing multilayered bovine serum albumin crosslinked with glutaraldehyde. *J Chromatogr A*. 1998;822:53–58.
10. Kuhn R, Hoffstetter-Kuhn S. Chiral separation by capillary electrophoresis. *Chromatographia*. 1992;34(9–10):505–512.
11. Schmitt T, Engelhardt H. Charged and uncharged cyclodextrins as chiral selector in capillary electrophoresis. *Chromatographia*. 1993; 37(9/19):475–481.
12. Valtcheva L, Mohammad J, Pettersson G, Hjertén S. Chiral separation of β-blockers by high-performance capillary electrophoresis based on non-immobilized cellulase as enantioselective protein. *J Chromatogr A*. 1993;638(2/28):263–267.
13. Takeuchi T, Horikawa R, Tanimura T. Enantioselective solvent extraction of neutral dl-amino acids in two-phase systems containing N-n-alkyl-L-proline derivatives and copper(II). *Anal Chem*. 1984;56: 1152–1155.
14. Bauer K, Falk H, Schlögl K. Racematspaltung von chiralen Ferrocenderivaten durch Gegenstrom. *Monatsh Chem*. 1968;99:2186–2194.
15. Bowman NS, McCloud GT, Schweitzer GK. Partial resolution of some organic racemates by solvent extraction. *J Am Chem Soc*. 1968;90(14):3848–3852.
16. Takeuchi T, Horikawa R, Tanimura T, Kabasawa Y. Resolution of DL valine by countercurrent solvent extraction with continuous sample feeding. *Sep Sci Technol*. 1990;25(7):941–951.
17. de Haan AB, Simádi B. Extraction technology for the separation of optical isomers. In: Yishak M, Kertes AS, editors. *Ion Exchange and Solvent Extraction: A Series of Advances, Vol. 15*. New York: Decker, 2001:255–294.
18. Schuur B, Floure J, Hallett AJ, Winkelman JGM, deVries JG, Heeres HJ. Continuous chiral separation of amino acid derivatives by enantioselective liquid–liquid extraction in centrifugal contactor separators. *Org Process Res Dev*. 2008;12:950–955.
19. Steensma M, Kuipers NJM, de Haan AB, Kwant G. Identification of enantioselective extractants for chiral separation of amines and aminoalcohols. *Chirality*. 2006;18:314–328.
20. Schuur B, Verkuijl BJV, Minnaard AJ, de Vries JG, Heeres HJ, Feringa BL. Chiral separation by enantioselective liquid-liquid extraction. *Org Biomol Chem*. 2011;9:36–51.
21. Tang KW, Chen YY, Liu JJ. Resolution of zopiclone enantiomers by biphasic recognition chiral extraction. *Sep Purif Technol*. 2008; 62:683–688.
22. Tang KW, Song LT, Liu YB, Pan Y, Jiang XY. Separation of flurbiprofen enantiomers by biphasic recognition chiral extraction. *Chem Eng J*. 2010;158:411–417.
23. Tang KW, Yi JM, Huang KL, Zhang GL. Biphasic recognition chiral extraction: a novel method for separation of mandelic acid enantiomers. *Chirality*. 2009;21:390–395.
24. Tang K, Miao J, Zhou T, Liu Y. Equilibrium studies on liquid-liquid reactive extraction of phenylsuccinic acid enantiomers using hydrophilic ß-CD derivatives extractants. *Chin J Chem Eng*. 2011;19(3): 397–403.
25. Li JH, Li FF. Chiral separation of α-cyclohexyl-mandelic acid by aqueous two phase system combined with Cu_2-ß-cyclodextrin complex. *Chem Eng J*. 2012;211:240–245.
26. Zhou CS, Xu P, Tang KW, Jiang XY, Yang T, Zhang PL. Enantioselective extraction of hydrophilic 2-chloromandelic acid enantiomers by hydroxyl-ß-cyclodextrin: experiments and modeling. *Chem Pap*. 2013;67(2):155–163.
27. Tang K, Chen Y, Huang K, Liu J. Enantioselective resolution of chiral aromatic acids by biphasic recognition chiral extraction. *Tetrahedron Asymmetry*. 2007;18:2399–2409.
28. Tang KW, Yi J, Liu Y, Jiang X, Pan Y. Enantioselective separation of R,S-phenylsuccinic acid by biphasic recognition chiral extraction. *Chem Eng Sci*. 2009;64:4081–4088.
29. Loftsson T, Másson M, Brewster ME. Self-association of cyclodextrins and cyclodextrin complexes. *J Pharm Sci*. 2004;93:1091–1099.
30. Holbach A, Caliskan E, Lee HS, Kockmann N. Process intensification in small scale extraction columns for counter-current operations. *Chem Eng Process*. 2014;80:21–28.
31. Davies M, Kybett B. Sublimation and vaporization heats of long-chain alkohols. *Transaction of the Faraday Society*. 1965;61:1608–1617.
32. Schuur B, Hallett AJ, Winkelman JGM, deVries JG, Heeres HJ. Scalable enantioseparation of amino acid derivatives using

continuous liquid-liquid extraction in a cascade of centrifugal contactor separators. *Org Process Res Dev*. 2009;13(5):911–914.
33. Schuur B, Winkelman JGM, de Vries JG, Heeres HJ. Experimental and modeling studies on the enantio-separation of 3,5 dinitrobenzoyl-(R),(S)-leucine by continuous liquid-liquid extraction in cascades of centrifugal contactor separators. *Chem Eng Sci*. 2010;65:4682–4690.
34. Tang K, Zhang H, Zhang P. Continuous separation of α-cyclohexyl mandelic acid enantiomers by enantioselective liquid-liquid extraction in centrifugal contactor separators: experiments and modeling. *Ind Eng Chem Res*. 2013;52:3893–3902.
35. Tang K, Zhang H, Liu Y. Experimental and simulation on enantioselective extraction in centrifugal contactor separators. *AIChE J*. 2013; 57(7):2594–2602.
36. Steensma M, Kuipers NJM, de Haan AB, Kwant G. Modelling and experimental evaluation of reaction kinetics in reactive extraction for chiral separation of amines, amino acids and amino alcohols. *Chem Eng Sci*. 2007;62:1395–1407.
37. Zhang P, Cai J, Tang K, Liu Y, Liu Y, Yan J. Equilibria and kinetics of reactive extraction of pranoprofen enantiomers from organic solution. *Chem Eng Process*. 2012;61:16–22.
38. Sleicher CA. Entrainment and extraction efficiency of mixer settlers. *AIChE J*. 1960;6(3):529–531.
39. Sleicher CA. Axial mixing and extraction efficiency. *AIChE J*. 1959; 5(2):145–149.

Manuscript received Aug. 25, 2014, and revision received Oct. 6, 2014.